

# Theory of the spatial structure of non-linear lasing modes

Hakan E. Türeci

*Institute of Quantum Electronics, ETH Zurich, 8093 Zurich, Switzerland*

A. Douglas Stone and Li Ge

*Department of Applied Physics, P. O. Box 208284,  
Yale University, New Haven, CT 06520-8284, USA*

(Dated: September 26, 2018)

A self-consistent integral equation is formulated and solved iteratively which determines the steady-state lasing modes of open multi-mode lasers. These modes are naturally decomposed in terms of frequency dependent biorthogonal modes of a linear wave equation and not in terms of resonances of the cold cavity. A one-dimensional cavity laser is analyzed and the lasing mode is found to have non-trivial spatial structure even in the single-mode limit. In the multi-mode regime spatial hole-burning and mode competition is treated exactly. The formalism generalizes to complex, chaotic and random laser media.

The steady-state electric field within and outside of a single or multi-mode laser arises as a solution of the non-linear coupled matter-field equations, the simplest of which are the two-level Maxwell-Bloch equations treated below. While the basic equations involved have been known for many years, and many aspects of their temporal dynamics have been studied [1], relatively little progress has been made in understanding the spatial structure of the non-linear electric field, particularly in the case of multi-mode solutions for which spatial hole-burning and other non-linear effects are critical. It is natural to attempt to understand the non-linear solutions in terms of solutions of a linear wave equation. The two standard choices are either the hermitian solutions of a perfectly reflecting (closed) passive laser cavity [2], or the non-hermitian non-orthogonal resonances of the open passive cavity [3, 4]). In fact the intuitive picture of a lasing mode is that it arises when one of the resonances of the passive cavity is “pulled” up to the real axis by adding gain to the resonator. Often comparison of the numerically generated lasing modes with calculated linear resonances do show strong similarities in spatial structure, providing useful interpretation of lasing modes [5, 6], although not a predictive theory. However with the current interest in complex laser cavities based on wave-chaotic shapes [7, 8], photonic bandgap media [9, 10] or random media [11, 12] it is important to have a quantitative and predictive theory of the lasing states, as the numerical simulations required to solve the time-dependent Maxwell-Bloch equations are time-consuming and not easy to interpret.

In recent work we have formulated a theory of steady-state multi-mode lasing which addresses these concerns [13]. The theory implies that the natural linear basis for decomposing lasing solutions is the dual set of biorthogonal states corresponding to constant outgoing and incoming Poynting vector at infinity at the lasing frequencies (referred to as “constant flux” (CF) states). Our theory shows that even in conventional lasers it is incorrect

to regard the lasing modes as corresponding to a single resonance of the passive cavity and that multiple spatial frequencies occur even when there is a single lasing frequency close to the frequency of a single passive cavity resonance. These multiple spatial frequencies arise because several CF states contribute to a single lasing mode. Note that biorthogonal modes have been used extensively in resonator theory [14] (notably for the case of unstable resonators) but have not previously been applied to multimode lasing theory. For multimode lasing the main difficulty is treating modal interactions and the related effects of spatial hole-burning [15]. We sketch below an efficient method for treating these effects exactly which can in principle be used in designing laser cavities to predict power output and tailor the mode spectrum of the laser. The techniques are illustrated for the simple case of a one-dimensional edge-emitting laser.

We begin with the semiclassical laser equations within the rotating wave and slowly-varying envelope approximations (see Ref. [13] for a derivation)

$$\dot{e} = \frac{i}{2\omega_a} \left[ \omega_a^2 + \frac{c^2}{n^2(\mathbf{x})} \nabla^2 \right] e + \frac{2i\pi\omega_a}{n^2(\mathbf{x})} p \quad (1)$$

$$\dot{p} = -\gamma_{\perp} p + \frac{g^2}{i\hbar} e D \quad (2)$$

$$\dot{D} = \gamma_{\parallel} (D_0 - D) - \frac{2}{i\hbar} (ep^* - pe^*) \quad (3)$$

describing a laser comprised of a uniform gain medium of two-level atoms (with level spacing  $\hbar\omega_a$ ) embedded in a background dielectric medium/cavity with arbitrary spatially varying index of refraction  $n(\mathbf{x})$ . Here  $e(\mathbf{x}, t)$ ,  $p(\mathbf{x}, t)$  are the envelopes of the field and polarization,  $D(\mathbf{x}, t)$  is the inversion,  $D_0$  is the pump strength,  $g$  is the dipole matrix element,  $\gamma_{\perp}$  and  $\gamma_{\parallel}$  are damping constants for  $p$ ,  $D$ . As usual the fast variation of the fields at  $\omega_a$  is removed and the actual fields are given by  $(E, P) = (e, p)e^{i\omega_a t} + c.c.$  For simplicity we take  $e$ ,  $p$  to be scalar fields, appropriate for the 1D case with TM polarization that we will discuss below; the same scalar form would

apply for planar random or chaotic cavities.  $n(\mathbf{x})$  is the (possibly) spatially dependent index of refraction of the cavity.

We assume a steady-state lasing solution which is multi-periodic in time:  $e(\mathbf{x}, t) = \sum_{\mu} \Psi_{\mu}(\mathbf{x})e^{-i\Omega_{\mu}t}$ ,  $p(\mathbf{x}, t) = \sum_{\mu} p_{\mu}(\mathbf{x})e^{-i\Omega_{\mu}t}$ . In contrast to standard modal expansions, not only the lasing frequencies  $\{\Omega_{\mu}\}$  but the spatial mode functions  $\{\Psi_{\mu}(\mathbf{x})\}$  are assumed to be unknown.

Such a multi-periodic solution requires that the inversion is approximately stationary [17], implying [13] that each lasing mode must satisfy the self-consistent equation.

$$\Psi_{\mu}(\mathbf{x}) = \frac{i\frac{4\pi\omega_{\mu}^2 g^2}{\hbar c^2} D_0}{-i\Omega_{\mu} + \gamma_{\perp}} \int_{\mathcal{D}} d\mathbf{x}' \frac{G(\mathbf{x}, \mathbf{x}'|\Omega_{\mu})\Psi_{\mu}(\mathbf{x}')}{1 + \sum_{\nu} g(\Omega_{\nu})|\Psi_{\nu}(\mathbf{x}')|^2} \quad (4)$$

where  $g(\Omega_{\mu})$  is the gain profile evaluated at the lasing frequency,  $\mathcal{D}$  is the cavity domain and  $G$  is the Green function of the cavity wave equation  $[\nabla^2 + n^2(\mathbf{x})k^2]G(\mathbf{x}, \mathbf{x}'|\omega) = \delta^3(\mathbf{x} - \mathbf{x}')$  with purely outgoing boundary conditions and  $k = \omega/c$  is an external wavevector of the lasing solution at infinity (for multimode solutions  $k = k_{\mu} = \Omega_{\mu}/c$ ). Henceforth we set  $c = 1$  and use wavevector and frequency interchangeably. With these non-hermitian boundary conditions the spectral representation  $G(\mathbf{x}, \mathbf{x}'|k)$  is of the form:

$$G(\mathbf{x}, \mathbf{x}'|k) = \sum_m \frac{\varphi_m(\mathbf{x}, k)\bar{\varphi}_m^*(\mathbf{x}', k)}{2\eta_m k_a(k - k_m)}. \quad (5)$$

Here the functions  $\varphi_m(\mathbf{x}, k)$  are the CF states which satisfy  $-\nabla^2\varphi_m(\mathbf{x}, k) = n^2(\mathbf{x})k_m^2\varphi_m(\mathbf{x}, k)$  with the non-hermitian boundary condition of only outgoing waves of wavevector  $k$  at the cavity boundary. For the special case of a 1D cavity of length  $a$  considered below (see Fig. 2, inset) this condition is just  $\partial_x\varphi_m(x)|_a = +ik\varphi_m(a)$ . Note this differs subtly but importantly from the quasi-bound state boundary condition where the complex eigenvalue  $k_m$  replaces the real wavevector  $k$  [13]. The dual set of functions  $\bar{\varphi}_m(x, k)$  satisfy the complex conjugate differential equation with the boundary conditions  $\partial_x\bar{\varphi}_m(x)|_a = -ik\bar{\varphi}_m(a)$  corresponding to constant incoming flux. In general these functions satisfy the biorthogonality relations [18]:  $\int_{\mathcal{D}} d\mathbf{x} \bar{\varphi}_m^*(\mathbf{x}, k)n^2(\mathbf{x})\varphi_n(\mathbf{x}, k) = \eta_m(k)\delta_{mn}$ , and are also complete. These relations make it possible to expand an arbitrary lasing solution

$$\Psi_{\mu}(\mathbf{x}) = \sum a_{\mu}^{\mu} \varphi_{\mu}^{\mu}(\mathbf{x}) \quad (6)$$

so that each  $\Psi_{\mu}$  is a vector in the space of biorthogonal functions. Here,  $\varphi_{\mu}^{\mu}(\mathbf{x}) = \varphi_m(\mathbf{x}, k_{\mu})$  and in what follows we define  $k_{\mu}^{\mu} = k_m(k_{\mu})$ . By substitution of (6) into

Eq. (4) and use of the biorthogonality relations one finds:

$$a_{\mu}^{\mu} = \frac{iD_0\gamma_{\perp}}{(\gamma_{\perp} - ik_{\mu})} \frac{1}{\eta_m^{\mu}(k_{\mu} - k_m^{\mu})} \times \int_{\mathcal{D}} \frac{d\mathbf{x} \bar{\varphi}_m^{\mu*}(\mathbf{x}) \sum_p a_p^{\mu} \varphi_p^{\mu}(\mathbf{x})}{1 + \sum_{\nu, q, r} g(k_{\nu}) a_q^{\nu} a_r^{\nu*} \varphi_q^{\nu}(\mathbf{x}) \varphi_r^{\nu*}(\mathbf{x})} \quad (7)$$

where we have rescaled the pump  $2\pi k_a g^2 D_0 / \hbar \gamma_{\perp} \rightarrow D_0$ , and measured electric field in units  $e_c = \hbar \sqrt{\gamma_{\parallel} \gamma_{\perp}} / 2g$ .

Equation (7) is the key result of our work; it determines the lasing mode(s), each of which is a superposition of CF states which depends on its lasing frequency,  $k_{\mu}$ , and the pump power,  $D_0$ . It is useful to regard Eq. (7) as defining a map of the complex vector space of coefficients  $\mathbf{a}^{\mu} = (a_1^{\mu}, a_2^{\mu}, \dots)$  into itself, where the actual non-zero lasing solution is a fixed point of this map. Above the lasing threshold for each mode,  $D_{0t}^{\mu}$ , we find that the non-zero solutions are stable fixed points and trial vectors flow to them under iteration of the map while the trivial zero solutions, which below  $D_{0t}^{\mu}$  are stable, become unstable. Note that the map is proportional to  $[k_{\mu} - k_m]^{-1}$ , favoring the CF state with complex wavevector close to the real lasing wavevector, and it is also proportional to  $[\gamma_{\perp} - ik_{\mu}]^{-1}$ , insuring that the lasing frequency is near the center of the gain profile. It can be shown that in the high-finesse limit in which the imaginary part of the CF frequency is very much smaller than the real spacing between them only one CF state dominates the lasing state (the "single-pole approximation"), and this CF state is virtually identical to the corresponding linear resonance [13]. In this limit the picture of a single resonance being "pulled" up to the real axis is valid. However in many realistic cases this limit is not realized and the actual lasing solution is the superposition of CF states determined by Eq. (7).

Eq. (7) determines the lasing frequencies as well. For the first lasing mode and a uniform index resonator this is particularly simple. At threshold the CF states in the denominator of the integrand can be ignored and biorthogonality leads to a simple relation:

$$a_m = \frac{iD_0\gamma_{\perp}/n^2}{(\gamma_{\perp} - ik)} \frac{1}{(k - k_m(k))} a_m. \quad (8)$$

For a non-trivial solution we must have  $a_m \neq 0$  for some  $m$  and hence the coefficient must be real and equal to unity. The reality condition determines that the possible lasing frequencies at threshold are  $k_t^{(m)} = \frac{\gamma_{\perp} q_m(k_t^{(m)})}{\gamma_{\perp} + \kappa_m(k_t^{(m)})}$  where  $k_m \equiv q_m(k) - i\kappa_m(k)$  (we suppress the index  $\mu$  here). Furthermore, the modulus unity condition determines the threshold pumping:

$$D_{0t}^{(m)} = n^2 \kappa_m \left[ 1 + \frac{q_m^2}{(\gamma_{\perp} + \kappa_m)^2} \right]. \quad (9)$$

The CF state  $m$  and associated frequency leading to the lowest threshold will be the first lasing mode. Note that

in contrast to the traditional mode-pulling formula [16] where the cavity mode frequency is a fixed value, here the single-mode laser frequency is determined by the solution of a self-consistent equation (a transcendental equation for the 1D case). Nonetheless for high finesse cavities this condition agrees with standard results: the lasing frequency is very close to the cavity resonance nearest to the gain center, pulled towards the gain center by an amount which depends on the relative magnitude of  $\gamma_{\perp}$  vs.  $\kappa_m$  (which is approximately the resonance linewidth) [13].

Above threshold the lasing mode is found by initially choosing the lasing wavevector,  $k = k_t^{(m)}$ , calculating the sets  $\{\varphi_m\}, \{\bar{\varphi}_m\}$  corresponding to that choice and then iterating Eq. (7) starting from a trial vector  $\mathbf{a}(0)$  to yield output  $\mathbf{a}(1)$ . A natural choice for the initial vector is  $a_m = 1, a_p = 0, \forall_p \neq m$ , where  $m$  is the dominant component at threshold, calculated from the above relations. As noted, the “lasing map” has the property that below the lasing threshold,  $D_{0t}$ , the iterated vector,  $\mathbf{a} \rightarrow \mathbf{0}$ , and above this threshold it converges to a finite value which defines the spatial structure of the lasing mode in terms of the CF states. There is one crucial addition necessary to complete the algorithm. Note that Eq. (7) is invariant under multiplication of the vector  $\mathbf{a}$  by a global phase  $e^{i\theta}$ , so iteration of (7) can never determine a unique non-zero solution. Therefore it is necessary to fix the “gauge” of the solution by demanding that we solve (7) with the constraint of a certain global phase (typically we take the dominant  $a_m$  to be real). Thus after each iteration of (7) we must adjust the lasing frequency to restore the phase of  $a_m$ ; it is just this gauge fixing requirement which causes the lasing frequency to flow from our initial guess to the correct value above threshold. The invariance of (7) under global phase changes guarantees that the frequency thus found is independent of the particular gauge choice. For multi-mode lasing we repeat this procedure for each vector  $\mathbf{a}^{\mu}$ . In the single-mode regime only one of these vectors will flow to a non-zero fixed point. This behavior of the multi-mode lasing map is illustrated in Fig. 1 for the simple uniform index 1D cavity corresponding to an edge-emitting laser with a perfect mirror at the origin and an index step at  $x = a$  (inset to Fig. 2). Below the first threshold, determined from Eq. 9 above, the entire set of vectors  $\mathbf{a}^{\mu}$  flow to zero; above that threshold the first lasing mode turns on and its intensity grows linearly with pump strength. Due to its non-linear interaction with other modes, the turn-on of the second and third lasing modes is dramatically suppressed, leading to a factor of four increase in the interval of single-mode operation. The intensity shows slope discontinuities at higher thresholds as seen in normal laser operation. Note that in this approach effects of spatial hole-burning and mode competition are treated exactly and not in the near-threshold approximation (cubic non-linearity) traditionally used [2, 16] which greatly

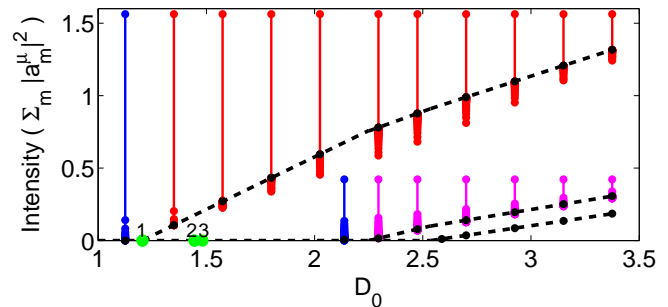


FIG. 1: Convergence and solution of the multimode lasing map for 1D resonator with  $n_0 = 1.5$ ,  $k_a = 19.89$  and  $\gamma_{\perp} = 4.0$  vs. pump  $D_0$ . Three modes lase in this range. At threshold they correspond to CF states  $m = 8, 9, 10$  with threshold lasing frequencies  $k_t^{(8)} = 18.08, k_t^{(9)} = 19.91$ , and  $k_t^{(10)} = 21.76$ , and non-interacting thresholds  $D_0^{(9)} = 1.204, D_0^{(10)} = 1.445, D_0^{(8)} = 1.482$  (green dots).  $k_t^{(9)} \approx k_a$  and  $m = 9$  has the lowest threshold. Due to mode competition, modes 2,3 do not lase until much higher values ( $D_0 = 2.25, 2.53$ ). Each mode is represented by an 11 component vector of CF states; we plot the sum of  $|a_m|^2$  vs. pump  $D_0$ . Below threshold the vectors flow to zero (blue dots). For  $D_0 \geq 1.204$  the sum flows (red dots) to a non-zero value (black dashed line), and above  $D_0 = 2.25, 2.53$ , two additional non-zero vector fixed points (modes) are found (convergence only shown for modes 1,2).

*underestimates* the output power [13].

We now consider the spatial structure of the CF states defining the lasing modes. The linear resonances (quasi-bound states) of this system are easily found [13], they are complex sine waves of wavevector  $n_0 k_m^{qb} a = \pi(m + 1/2) - i/2 \ln[(n_0 + 1)/(n_0 - 1)]$ . The constant linewidth  $Im[k_m^{(qb)}] \equiv -\kappa_m^{(qb)}$  follows from the Fresnel transmissivity of dielectric boundary at normal incidence. Note that  $\kappa_m^{(qb)} > 0$  here, corresponding to amplification with increasing  $x$ . From Eq. (6) we expect the lasing mode to involve several CF states and differ most from a single cavity resonance for a low finesse cavity; thus we consider relatively small index,  $n_0 = 1.5$ . The CF states depend on the lasing wavevector,  $k$ . In Fig. (2) we choose it to be the real part of the wavevector of the 9<sup>th</sup> resonance,  $k_9^{qb}$ , and plot the 7 closest CF eigenvalues,  $k_m$  (inset, Fig. 2). The 9<sup>th</sup> CF state has  $k_9 \approx k_9^{qb}$  and within the cavity is very close to the  $m = 9$  resonance [13], but the other  $k_m$ , while they have  $Re[k_m] \approx Re[k_m^{(qb)}]$  (hence similar FSR) have substantially larger or smaller  $\kappa_m$  than  $\kappa_m^{(qb)}$ . Hence only the  $m = 9$  CF state is close to a linear resonance, emphasizing that CF states are *not* resonances. We plot several of these states in Fig. 2, showing their different amplification rates. The actual lasing mode will be the sum of several of these CF modes with different spatial frequencies and amplification rates. In Fig. (3) we plot such a mode. Standard modal expansions in laser theory are equivalent to choosing only the

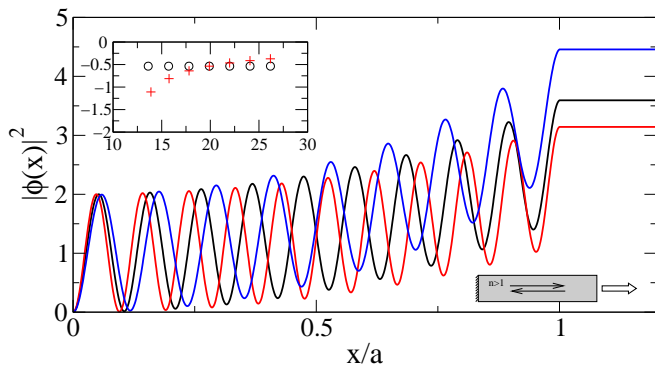


FIG. 2: The spatial structure of three consecutive CF modes calculated at the external frequency  $k = 19.90$  and  $n_0 = 1.5$ . The CF frequencies are  $k_m = 19.90 - 0.536i$  (black),  $21.99 - 0.466i$  (red), and  $17.81 - 0.640i$  (blue). The upper inset compares the CF mode frequencies (+) with the quasi-bound mode frequencies (o) in the range  $m = [6, 12]$ . Lower inset: schematic of the edge-emitting laser cavity.

central CF state and missing the contribution of these spatial “side-bands” [13]. The inset to Fig. 3 shows that near threshold only one CF state dominates (one can show that the other components are of order the cube of the dominant component). But well above threshold the two nearest neighbor CF states are each 15% of the main component and since one of these has higher amplification rate, the final effect is to increase the output power by more than 43% (see Fig. 3). The sidebands are still 6% of the dominant component when the index is increased to  $n_0 = 3$ , leading to an increase in output power by 26% (see inset, Fig. 3). The formalism

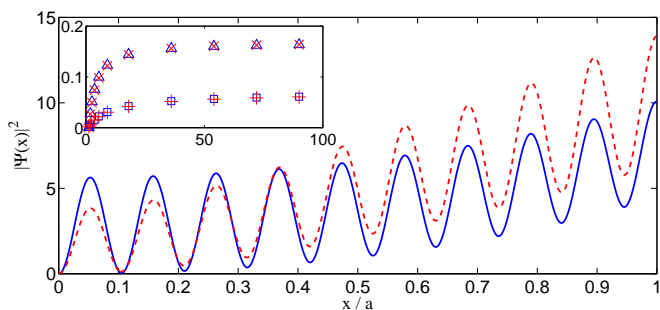


FIG. 3: Non-linear electric field intensity for a single-mode edge-emitting laser with  $n_0 = 1.5$ ,  $k_a = 19.89$ ,  $\gamma_{\perp} = 0.5$ ,  $D_0 = 9$ . The full field (red line) has an appreciably larger amplitude at the output  $x = a$  than the “single-pole” approximation (blue) which neglects the sideband CF components. Inset: The ratio of the two largest CF sideband components to that of the central pole for  $n_0 = 1.5$  ( $\square$ ,  $\times$ ) and  $n_0 = 3$  ( $\square$ ,  $+$ ) vs. pump strength  $D_0$ .

we have presented here is ideal for treating random or

wave-chaotic lasers for which the output directionality, output power and mode spectrum are very hard to predict with heuristic arguments. Moreover in these systems the finesse typically is parametrically smaller than unity, suggesting that each lasing mode will consist of many CF states without a dominant component. We have considered here the borderline case of a cavity with finesse of order unity, so there is a dominant CF component, but the spatial sidebands are still appreciable. Since our method treats the non-linearity and mode-competition exactly we anticipate that it may be useful in designing efficient semiconductor microcavity lasers.

This work was supported by NSF grant DMR 0408636 and by the Aspen Center for Physics.

- 
- [1] P. Mandel, *Theoretical problems in cavity nonlinear optics* (Cambridge University Press, Cambridge, UK, 1997).
  - [2] H. Haken, *Light (Volume 2)* (North-Holland Physics Publishing, Amsterdam, Netherlands, 1985).
  - [3] P. T. Leung, S. Y. Liu, and K. Young, *Phys. Rev. A* **49**, 3057 (1994).
  - [4] E. S. C. Ching, P. T. Leung, A. M. van den Brink, W. M. Suen, S. S. Tong, and K. Young, *Rev. Mod. Phys.* **70**, 1545 (1998).
  - [5] T. Harayama, P. Davis, and K. S. Ikeda, *Phys. Rev. Lett.* **90**, 063901 (2003).
  - [6] T. Harayama, S. Sunada, and K. S. Ikeda, *Phys. Rev. A* **72** 013803 (2005).
  - [7] H. E. Türeci, H. G. L. Schwefel, P. Jacquod, and A. D. Stone, *Progress In Optics* **47**, 75 (2005).
  - [8] H. G. L. Schwefel, H. E. Türeci, A. D. Stone, and R. K. Chang, in *Optical Processes*, edited by K. J. Vahala (World Scientific, 2004).
  - [9] O. Painter, R. K. Lee, A. Scherer, A. Yariv, J. D. O’Brien, P. D. Dapkus, and I. Kim, *Science* **284**, 1819 (1999).
  - [10] H. Y. Ryu, S. H. Kim, H. G. Park, J. K. Hwang, Y. H. Lee, and J. S. Kim, *Applied Physics Letters* **80**, 3883 (2002).
  - [11] H. Cao, *Waves In Random Media* **13**, R1 (2003).
  - [12] H. Cao, *Journal Of Physics A-Mathematical And General* **38**, 10497 (2005).
  - [13] H. E. Türeci, A. D. Stone, and B. Collier, *Phys. Rev. A* **74**, 1 (2006).
  - [14] A. E. Siegman, *Lasers* (University Science Books, Mill Valley, California, 1986).
  - [15] H. Haken and H. Sauermann, *Z. Phys.* **173**, 261 (1963).
  - [16] M. Sargent III, M. O. Scully, and W. E. Lamb Jr., *Laser Physics* (Addison-Wesley, Massachusetts, USA, 1974).
  - [17] H. Fu and H. Haken, *Phys. Rev. A* **43**, 2446 (1991).
  - [18] P. M. Morse and H. Feshbach, *Methods of Theoretical Physics, Part I* (McGraw-Hill, New York, NY, USA, 1953).